The 8th European Congress on Computational Methods in Applied Sciences and Engineering
ECCOMAS Congress 2022
5-–9 June 2022, Oslo, Norway

THE INTERACTION BETWEEN AN ISOLATED ROUGHNESS ELEMENT AND FREE-STREAM TURBULENCE

M. GHOLAMISHEERI, K. DUROVIC, S. B. MAMIDALA, J. H. M. FRANSSON, A. HANIFI, AND D. S. HENNINGSON

FLOW, Engineering Mechanics, KTH Royal Institute of Technology, Stockholm, Sweden
e-mail: masumeh, kdj, mamidala, jensf, hanifi, henning@kth.se

Key words: Free-stream Turbulence, Roughness Induced Transition

Abstract. Control and delay of the laminar-turbulent transition is a key parameter in reducing skin friction and drag. The flow characteristics, surface roughness, and environmental noise can affect the onset of transition. The present work investigates, numerically and experimentally, the interaction of the free-stream turbulence (FST) and an isolated cylindrical roughness element, and the resulting impact on the transition onset in a flat-plate boundary layer. High-fidelity direct numerical simulations (DNS) are performed for a roughness element immersed in the boundary layer over a flat plate with an asymmetrical leading edge, with and without FST. The numerical results are compared to hot-wire anemometry measurements performed in the Minimum Turbulence Level wind tunnel at KTH. The initial numerical and experimental results show that in the absence of FST, for the chosen flow parameters, high- and low-speed streaks are generated downstream of the roughness element while the flow remains laminar and globally stable. When FST is added, the spanwise spacing of the streaky structures changes and the transition location of the boundary layer moves upstream. It was found that the aspect ratio of the streaky structures does not vary significantly.

1 INTRODUCTION

To improve performance of an aircraft and reduce its environmental footprints, one solution is to reduce the skin friction over the surface of the aircraft which stands for about 50% of the total drag. As the skin friction increases drastically when flow becomes turbulent, an effective approach to reduce the drag is to delay the laminar-turbulent transition. As evaluated by Schrauf [1], the total drag would be reduced by approximately 16% if the laminar flow is maintained on 40% of the nacelles, wings and other lifting surfaces of an aircraft. The onset of transition is highly dependent on the characteristics of the flow and geometry, e.g. free-stream turbulence intensity and length scales, environmental noise, and surface roughness.

The surface irregularities, if used in a controlled manner, can delay the laminar-turbulent transition and reduce the drag. This method has been studied for the flow cases corresponding to both swept and straight wings, see e.g. [2, 3, 4]. The effects of the roughness elements on the transition onset can be twofold. The generated streaks inside the boundary layer may make it more resistant to transition to turbulence. The combination of the aspect ratio of the surface roughness and the flow characteristics determines the delay or promotion of transition. A critical issue for the transition control by means of distributed roughness elements is its sensitivity to the level of free-stream turbulence (FST) and its length scales. Further, the roughness elements with aspect ratios beyond a certain threshold can promote the transition and hence increase the drag. Therefore, the geometrical parameters of roughness elements such as height, shape, aspect ratio and also spacing between them have to be chosen carefully.

The incoming flow may have different turbulence intensities depending on the operational environment. The presence of FST has a great impact on the transition process and its path in the boundary-layer flows. In the boundary-layer flows subjected to high FST intensities (larger than 1%) streamwise elongated structures with alternating high and low velocities appear [5, 6]. In these cases, transition occurs due to instability and breakdown of these streaks. These structures are similar to those generated by the surface roughness elements. The response of the boundary-layer flows to FST and roughness elements has been thoroughly investigated over the past few decades [7, 8, 9, 10], however, studies on the combined effect of the two components are rare [11, 12]. Therefore, the present study targets this topic combining numerical and experimental approaches.

In a recent publication, Fransson and Shahinfar [10] showed that the aspect ratio of the streaks generated by FST correlates with the FST Reynolds number, Re_{FST}, where,

$$Re_{FST} = \frac{u_{rms}\Lambda_x}{\nu} = Tu \cdot Re_\Lambda \,, \quad \text{and} \quad Re_\Lambda = \frac{U_\infty \Lambda_x}{\nu} \,. \tag{1}$$

Here, u_{rms} is the root-mean-square value of the velocity fluctuations, Tu denotes the FST intensity, Λ_x is the streamwise integral length scale, U_∞ represents the free-stream velocity, and ν is the kinematic viscosity of the flow. This indicates that the two main parameters affecting the perturbations that enter the boundary layer and consequently influence the transition onset are turbulence intensity and integral length scale. However, the influence of roughness element on the variation of aspect ratio of the streaks is unknown.

This paper is organized into four sections. The experimental setup is discussed in §2. In §3, the numerical specifications of the DNS simulations are introduced. Results from the com-

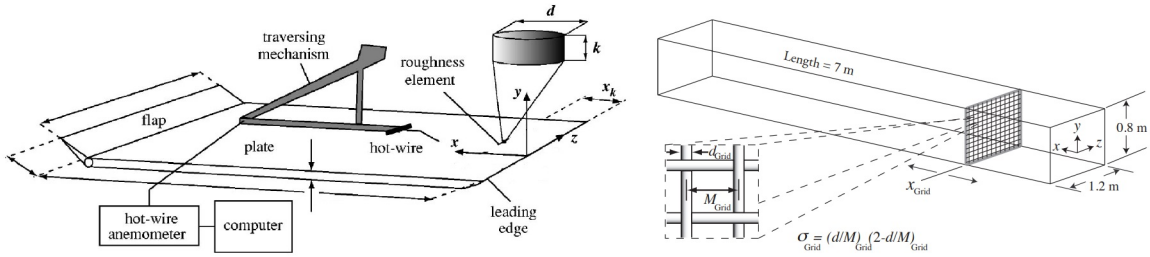

(a) (b)

Figure 1: (a) Experimental setup, showing the traverse system over the plate and roughness element location [13], and (b) the turbulence generating grid installed in the tunnel. Flap length: 450 mm, total plate length: 4360 mm, $x_k = 480$ mm, flap width: 1200 mm.

parison between the experimental measurements and DNS are reported in detail in §4. Finally, conclusions are drawn and key results are summarized in §5.

2 EXPERIMENTAL SETUP

The experimental measurements are performed in the minimum turbulence level (MTL) wind tunnel at KTH. The test section is 7 m long and has a cross section of 0.8 m × 1.2 m, (height × width). The installation of a trailing flap and the use of adjustable ceiling enable us to get a zero-pressure gradient boundary-layer flow over the plate with a relatively short negative pressure gradient or accelerating flow around the leading-edge region being measured. For velocity signal measurements, Hot-Wire-Anemometery (HWA) is employed. To generate FST, turbulent generating grids are installed upstream of the plate leading edge. The turbulence intensity is proportional to the pressure drop over the grid, which is given by the grid solidity ($\boldsymbol{\sigma}$) [10]. The FST length scales are function of the mesh width (M) and bar diameter (d) of the grid, see Figure 1.

In order to choose the simulation conditions, a few experimental measurements were conducted based on which a roughness Reynolds number equal to $Re_{hh} = U_h h/\nu = 244$ was chosen for the present study. Further, based on the size and location of the roughness element, the freestream velocity was set to 6.38 m/s. The initial experiments also suggest that with the chosen velocity and roughness aspect ratio, the flow over the roughness element remains laminar.

3 NUMERICAL SPECIFICATIONS

3.1 Method

The dynamics of a three-dimensional incompressible flow is described by the Navier-Stokes equations which reads as:

$$\mathbf{u}_t + (\mathbf{u}\cdot\nabla)\mathbf{u} = -\nabla p + \frac{1}{Re}\nabla^2\mathbf{u}\,, \tag{2}$$

$$\nabla\cdot\mathbf{u} = 0\,, \tag{3}$$

where, $\mathbf{u}$, p and Re are the velocity vector, pressure and the free-stream Reynolds number, respectively.

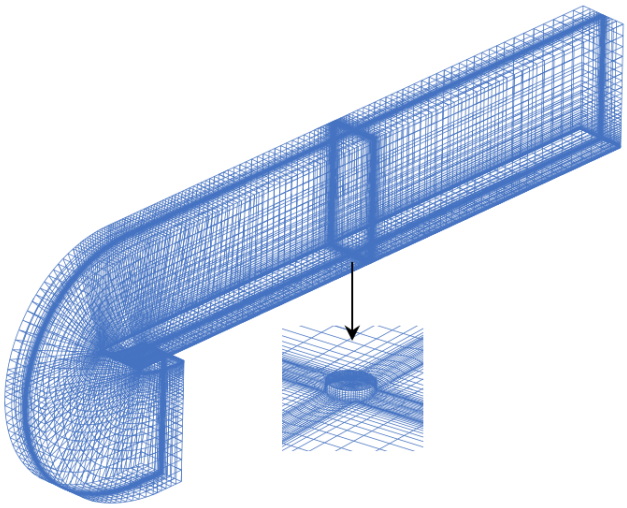

Figure 2: Schematic of the plate and the roughness location along with the structured mesh of hexahedral elements.

In the present study, Nek5000 [14], an open-source solver based on spectral element method (SEM) is used to solve the Navier-stokes equations. The numerical solution is expanded in each element using polynomials of order 9 on the Gauss-Lobatto-Legendre (GLL) quadrature points. The number of spectral elements in the structured mesh, see Figure 2, is 325000 which leads to 325 million degrees of freedom (i.e. total number of the GLL points). For time integration, a backward differentiation scheme of order 3 combined with an extrapolation of the same order (together called BDF3/EXT3) is employed.

3.2 Geometry

The plate leading edge is located at approximately $L_{le} = 34d$ downstream of the computational domain's inlet plane and the roughness element is placed at $80d$ downstream of the plate leading edge, centered in the spanwise direction. The roughness element has the diameter $d = 6\,\text{mm}$ and height $h = 1.3\,\text{mm}$ which gives the aspect ratio $\eta = d/h > 2.0$. The computational domain size is chosen to be $L_x = 200d$, $L_y = 33d$ and $L_z = 13d$ in the streamwise, wall-normal and spanwise directions, respectively. A schematic of the computational domain is shown in Figure 2.

The boundary conditions are specified as follows: a Dirichlet boundary condition for velocity is set for the inlet, a Neumann zero-pressure condition is chosen for the outlet, and no-slip condition is set at the wall. For the upper part of the domain, zero velocity in the directions parallel to the boundaries are considered (mixed outflow condition) and the two sides of the domain are periodic. Hereafter, the first simulation case which is without any free-stream turbulence is called "baseflow". In the second simulation case referred to as by "FST" simulation, isotropic and homogeneous free-stream turbulence is imposed as the Dirichlet boundary condition at the inlet of the plane. The disturbance field is a superposition of the Fourier modes with a random phase shift. Further information on the generation of free-stream turbulence can be found in

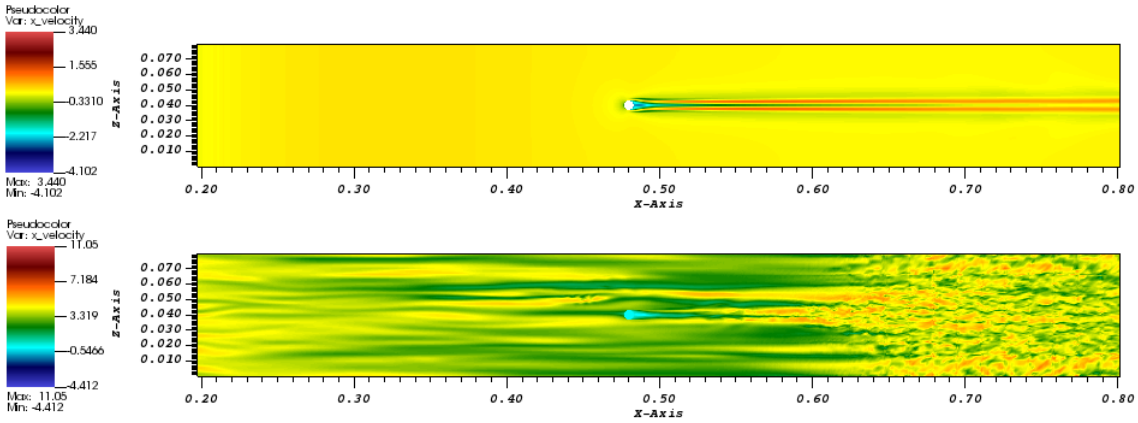

Figure 3: (Top) Contours of high- and low-speed streaks generated downstream of the roughness element without FST, and (bottom) the streaky structures and turbulent transition downstream of the roughness element when FST is imposed. The data are obtained from DNS.

Ref. [6].

4 RESULTS

4.1 Flow behaviour in the absence of FST

In this section, the results of simulation and experimental measurements of the baseflow case are compared where the flow over the plate is considered without imposing the FST. As expected, with the chosen free-stream velocity and the roughness aspect ratio, the flow remains laminar over the entire plate while high- and low-speed streaks are generate behind the roughness element. These streaks are shown through the velocity contour plot in Figure 3 (top).

For this case, the velocity profiles along the span of the wake behind the roughness as well as the evolution of the streaks are shown in Figure 4(top). Moving away from the wall, the velocity profiles for three y/δ locations are presented. The central wake and the surrounding high- and low-speed streaks are clearly strong inside the boundary layer. In contrast, outside of the boundary layer the wake and streak effects start to fade away.

To examine the stability of the flow in the presence of the roughness element, impulse response analysis is performed. An initial perturbation (wave-packet-like disturbance) is introduced upstream of the roughness element where the energy is centered in 2D modes:

$$(\mathbf{u}, \mathbf{v}, \mathbf{w}) = (\psi_{\mathbf{x}}, \psi_{\mathbf{y}}, 0) \quad \text{where} \quad \psi = \varepsilon \overline{\mathbf{x}} \cdot \overline{\mathbf{y}}^3 \exp(-\overline{\mathbf{x}}^2 - \overline{\mathbf{y}}^2 - \overline{\mathbf{z}}^2). \tag{4}$$

The energy growth versus the group velocity $C_g = (x - x_0)/t$ is shown in Figure 4(bottom). Here, the energy of the propagating modes is integrated over $y - z$ planes. To find the group velocity, an origin is defined at $16d$ upstream of the roughness and the reference velocity is $U_0 = 6.38\,\mathrm{m/s}$. The leading velocity of these propagating modes is observed to be less than 0.5 m/s. Consequently, the flow is found to be convectively unstable (i.e. globally stable).

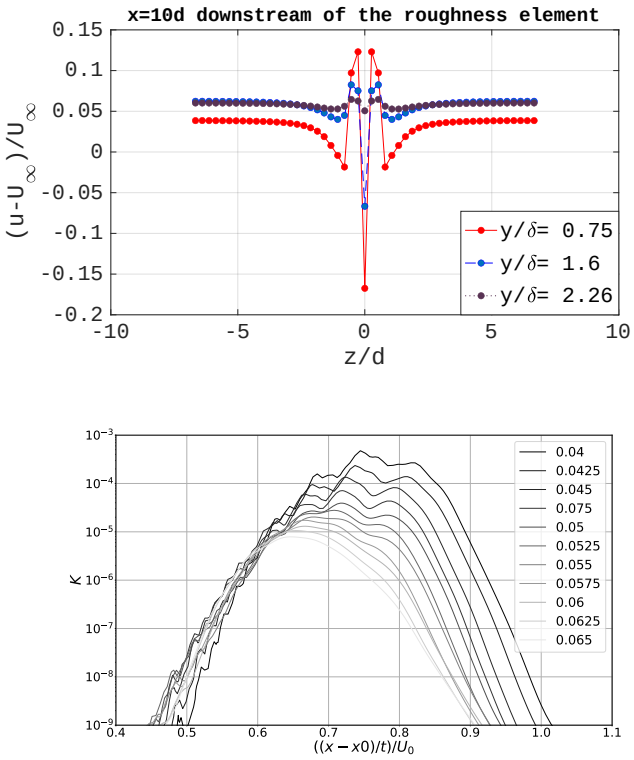

Figure 4: (top) Velocity profiles along the span, at the location of $x = 10\,d$ downstream of the roughness, and (bottom) the energy of the wave packet versus the group velocity. Note that the wall is located at $y = 0$.

4.2 Effects of FST

It is known that the turbulence characteristics such as intensity and length scales affect the downstream flow dynamics and boundary layer transition (see e.g. [10]). Therefor, to properly simulate the behaviour of turbulent flow, the parameters set at the inflow should be as identical as possible to the parameters defined in the wind tunnel. The spanwise-averaged distributions of the DNS turbulence intensity and length scale at the leading edge are shown in Figure 5. The averaged values are made over 30 points in the span and are used as a basis for the selection of the turbulence-generating grid in the wind tunnel. A snapshot of the generated flow inside the boundary layer is shown in Figure 3 (bottom), where the streaks are clearly visible. Further, the spacing between the streaks upstream of the roughness element is used as another characteristic parameter to match with the experiment, see Figure 6. Here, the half-streak spacing is calculated as the first minimum of two-point correlation in the spanwise direction at $x = 12d$ upstream of the roughness. It should be noted that the half-streak spacing at other locations upstream of the roughness element were also calculated, however no variation was observed. Instantaneous velocity field in a $y-z$ cross section is shown in Figure 6(b), to illustrate the high- and low-speed streaks along the span. Here, the baseflow velocity field (i.e. from the simulation without FST)

is subtracted from the instantaneous field in order to elucidate the streaks.

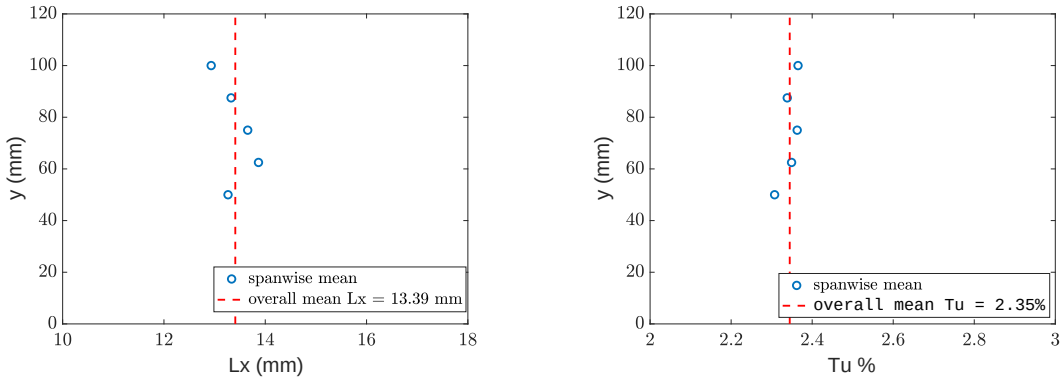

(a) (b)

Figure 5: Spanwise-averaged distributions of (a) turbulent intensity and (b) length scale at the leading edge extracted from the DNS results.

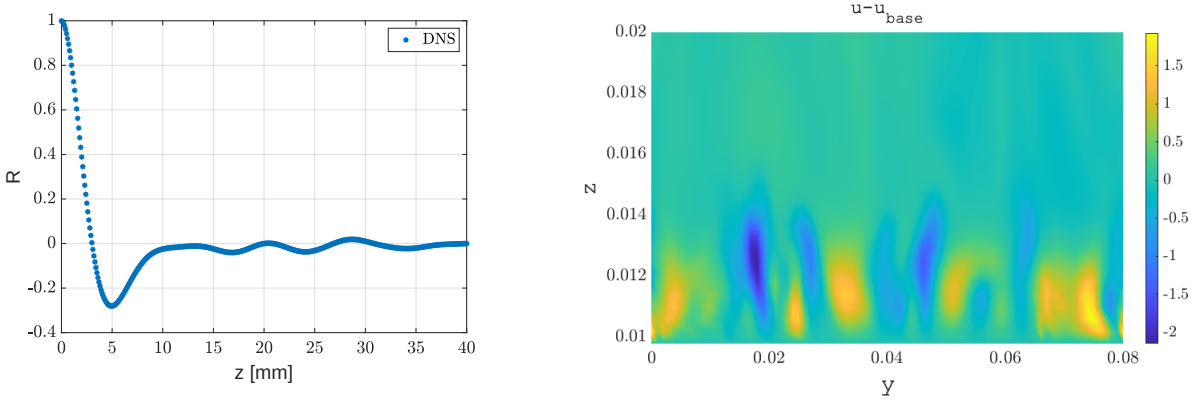

(a) (b)

Figure 6: (a) The two-point spanwise correlation of the streamwise velocity at $x = 12\,d$ upstream of the roughness, and (b) contour plot of the streaks (baseflow is subtracted from the FST simulation instantaneous snapshot) at $x = 12\,d$ upstream of the roughness.

The laminar-turbulent transition and the structures generated downstream of the roughness are shown through the contour plots of the streamwise velocity, in Figure 7. Here, to have a better representation of the FST generated streaks, the velocity of the baseflow simulation is subtracted from the streamwise velocity of the FST simulation. Wake is generated downstream of the roughness followed by the turbulent structures that spread in the span as the flow moves downstream.

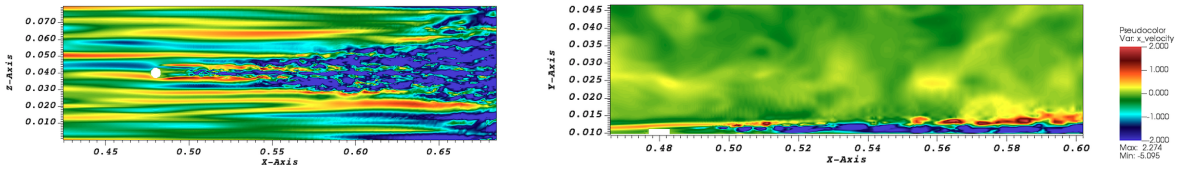

Figure 7: Contour plots of the streamwise velocity at cross sections located at (left) $y = 1.2\,\mathrm{mm}$ above the plate, and (right) at $z = 0$. Both plots have the same colorbar.

4.3 Comparison between DNS and experiment

The profiles of the time-averaged velocity and perturbations (i.e. $\overline{\mathbf{U}}$ and $\overline{\mathbf{u'}}$) from the DNS and the measurements are compared in Figure 8. The plots are shown consecutively from $2\,d$ to $12\,d$ downstream of the roughness. Closer to the boundaries ($z = 6\,d$ from the centre-line), and up to $4\,d$ downstream of the roughness, the averaged velocity and perturbation fields match well. However, further downstream and also at the roughness centre-line, where the flow transitions to turbulence, there is a deviation between experiment and DNS results, mainly in the velocity fluctuation fields. In addition, a comparison between the time-averaged velocity and associated fluctuations is made through contour plots, see Figure 9. Two cross sections, one closer to the roughness element, i.e. at $x = 2.5\,d$ and the other, further downstream at $x = 6\,d$, are represented. As inferred from the DNS, the two low-speed streaks merge together shortly downstream of the roughness and the fluctuations are stronger closer to the roughness element. These contour plots affirms that the transition event predicted by DNS is slightly further upstream and also closer to the roughness element.

One of the purposes of the current study is to find the correlation between the roughness element size and the streak spacing. For this, the half-streak spacing is found through the cross correlation of velocity signal in the spanwise direction. In Figure 10, DNS data at two upstream locations $-12\,d$ and $-6\,d$ as well as five downstream locations from $2\,d$ to $12\,d$ are shown by solid lines and the experimental measurements at two locations, $-12\,d$ and transition onset ($8.8d$) are represented by markers. Based on the plots, the roughness element is found to only slightly affect the streak-spacing. Further, the variation in the streak-spacing upstream and downstream of the roughness is very moderate.

The one-dimensional energy spectra from the streamwise velocity signal, in the free stream is plotted in Figure 11. The stream-wise location that is chosen to extract the data is at $x = 70d$ downstream of the roughness where the flow is found to be fully turbulent. There is a fair agreement between the DNS and experiment. It is noteworthy that the geometry does not have any periodic direction and as a result, the FFT (fast fourier transform) is only performed on time.

5 SUMMARY AND CONCLUSIONS

The influence of free-stream turbulence on the boundary layer over a flat plate in the presence of an isoilated cylindrical roughness element has been investigated through high-fidelity DNS and experimental measurements. To make a fair comparison between the DNS and experimental measurements, main free-stream characteristics, i.e. the integral length scale and turbulent

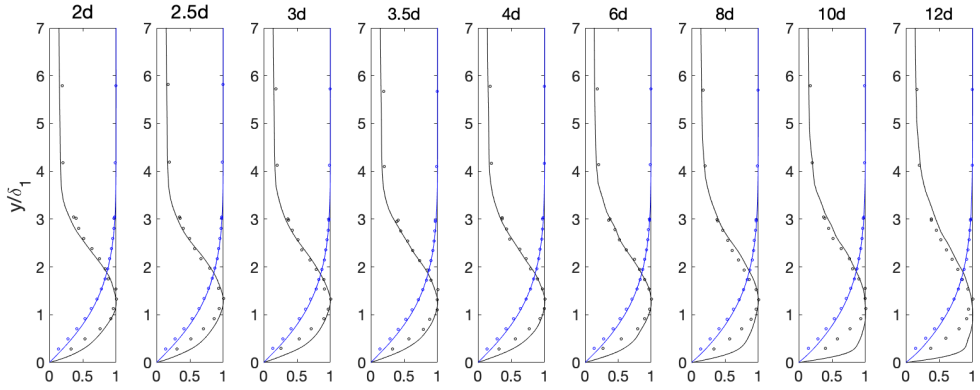

(a) $z = 6d$

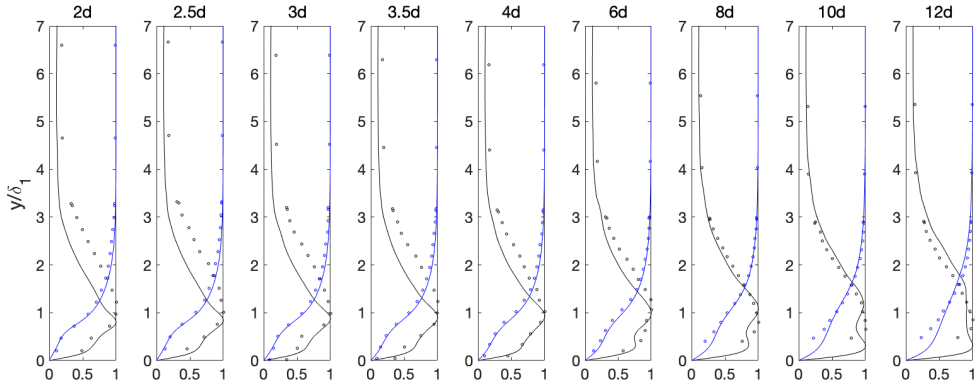

(b) $z = 0d$

Figure 8: The profiles of time-averaged streamwise velocity (blue) and corresponding velocity fluctuation (black): DNS (—) and Experiment (•).

intensity as well as the pressure gradient along the plate have been matched.

The baseflow results, i.e. the flow with no free-stream turbulence (FST) indicates that for the chosen free-stream velocity and roughness element heigh and aspect ratio ($\eta > 2.0$), the flow remains laminar and globally stable along the plate. Comparison of the flow field and velocity profiles for the FST simulation and experiment showed good overall agreement, while some discrepancies in the fluctuation fields further downstream of the roughness are observed. Even though the nominal inflow conditions were set the same in both simulation and experiments, the small differences between the synthetic inflow fluctuations and actual ones lead to different characteristics of the flow evolved downstream. These differences also affect the transition onset. The onset of transition predicted by DNS is found to be closer to the roughness element, however, the transition onset is varying along the span. A fair agreement is observed between the energy spectra of the streamwise velocity computed from the DNS and the experiment in the fully-turbulent region of the flow downstream of the roughness.

From the two-point spanwise correlation of streamwise velocity, streak spacing is calculated

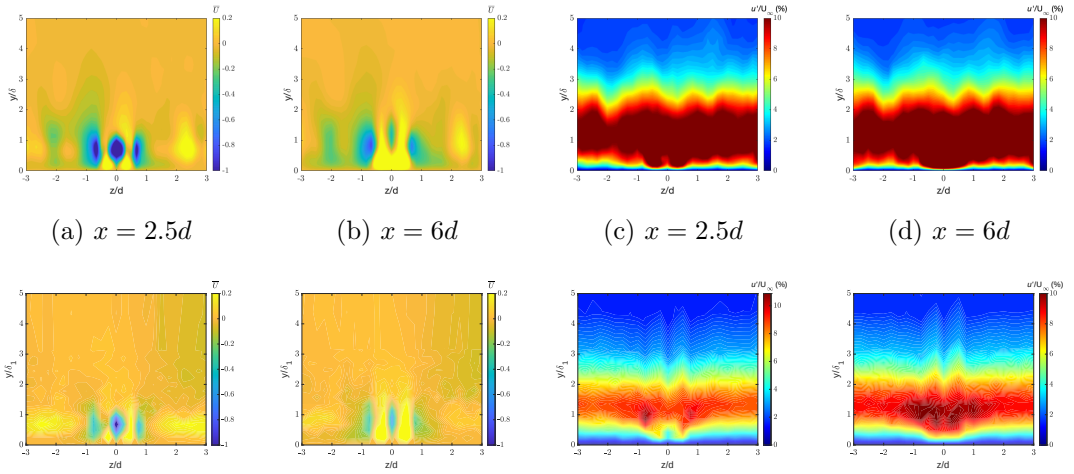

(a) $x = 2.5d$ (b) $x = 6d$ (c) $x = 2.5d$ (d) $x = 6d$

(e) $x = 2.5d$ (f) $x = 6d$ (g) $x = 2.5d$ (h) $x = 6d$

Figure 9: Contour plots of the time-averaged streamwise velocity and streamwise velocity fluctuation at $x = 2.5\,d$ and $6\,d$: DNS (a-d) and experiment (e-h).

which shows that the roughness element (with the height and radius adopted in this study) does not affect the streak spacing. To investigate the effect of roughness on streak spacing, if any, a parametric study for the free-stream condition and roughness size is needed.

REFERENCES

[1] G Schrauf. Status and perspectives of laminar flow. Aeronautical J., 109(1102):639–644, 2005.

[2] Jens H. M. Fransson, Alessandro Talamelli, Luca Brandt, and Carlo Cossu. Delaying transition to turbulence by a passive mechanism. Phys. Rev. Lett., 96:064501, Feb 2006.

[3] William S Saric, Andrew L Carpenter, and Helen L Reed. Passive control of transition in three-dimensional boundary layers, with emphasis on discrete roughness elements. Philosophical Transactions of the Royal Society A: Mathematical, Physical and Engineering Sciences, 369(1940):1352–1364, 2011.

[4] Seyed M. Hosseini, David Tempelmann, Ardeshir Hanifi, and Dan S. Henningson. Stabilization of a swept-wing boundary layer by distributed roughness elements. Journal of Fluid Mechanics, 718:R1, 2013.

[5] M. Matsubara and P. H. Alfredsson. Disturbance growth in boundary layers subjected to free-stream turbulence. Journal of Fluid Mechanics, 430:149–168, 2001.

[6] Luca Brandt, Philipp Schlatter, and Dan S. Henningson. Transition in boundary layers subject to free-stream turbulence. Journal of Fluid Mechanics, 517:167–198, 2004.

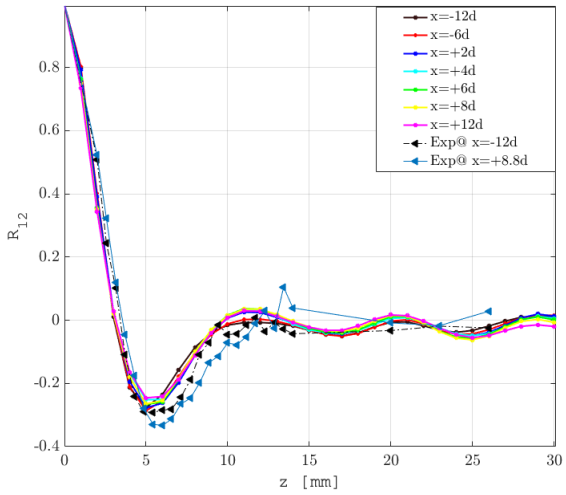

Figure 10: The cross correlation functions in the spanwise direction based on the DNS and experimental data.

[7] Philipp Schlatter, Luca Brandt, HC De Lange, and Dan S Henningson. On streak breakdown in bypass transition. Physics of fluids, 20(10):101505, 2008.

[8] Jens HM Fransson, Luca Brandt, Alessandro Talamelli, and Carlo Cossu. Experimental and theoretical investigation of the nonmodal growth of steady streaks in a flat plate boundary layer. Physics of Fluids, 16(10):3627–3638, 2004.

[9] Jean-Christophe Loiseau, Jean-Christophe Robinet, Stefania Cherubini, and Emmanuel Leriche. Investigation of the roughness-induced transition: global stability analyses and direct numerical simulations. Journal of Fluid Mechanics, 760:175–211, 2014.

[10] Jens H. M. Fransson and Shahab Shahinfar. On the effect of free-stream turbulence on boundary-layer transition. Journal of Fluid Mechanics, 899:A23, 2020.

[11] Seyed M. Hosseini, Ardeshir Hanifi, and Dan S. Hennigson. Effect of freestream turbulence on roughness-induced crossflow instability. Procedia IUTAM, 14:303–310, 2015.

[12] Luca De Vincentiis, Dan S. Henningson, and Ardeshir Hanifi. Transition in an infinite swept-wing boundary layer subject to surface roughness and free-stream turbulence. Journal of Fluid Mechanics, 931:A24, 2022.

[13] Jens H. M. Fransson, Luca Brandt, Alessandro Talamelli, and Carlo Cossu. Experimental and theoretical investigation of the nonmodal growth of steady streaks in a flat plate boundary layer. Physics of Fluids, 16(10):3627–3638, 2004.

[14] Nek5000 Version 17. Argonne National Laboratory, Illinois. https://nek5000.mcs.anl.gov.

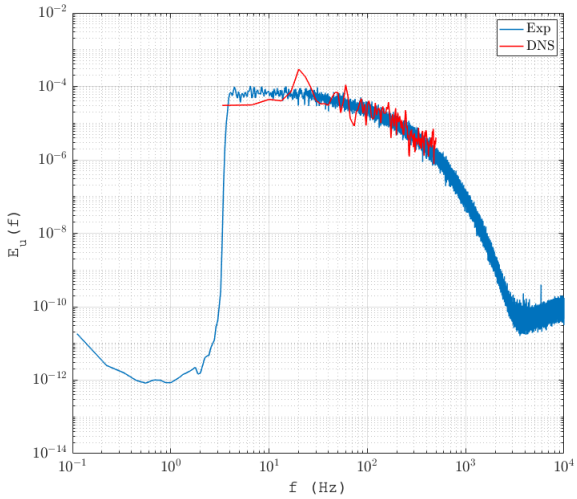

Figure 11: One-dimensional energy spectrum of the streamwise velocity signal computed at $x = 70\,d$ downstream of the roughness using the data of the DNS and experimental measurements.